ELSEVIER

Journal of Neuroscience Methods 157 (2006) 230–237

JOURNAL OF NEUROSCIENCE METHODS

www.elsevier.com/locate/jneumeth

Reverse correlation of rapid calcium signals in the zebrafish optic tectum in vivo

Pavan Ramdya [a,*], Bettina Reiter [b], Florian Engert [b]

[a] *Program in Neuroscience, Department of Neurobiology, Harvard Medical School, Boston, MA 02115, United States*
[b] *Department of Molecular and Cellular Biology, Harvard University, Cambridge, MA 02138, United States*

Received 8 March 2006; received in revised form 18 April 2006; accepted 25 April 2006

Abstract

Reverse correlation techniques provide a quantitative means of computing neuronal input/output relationships. Until now these methods have been limited to electrically recorded responses since unprocessed optical signals generally lack necessary temporal characteristics. We sought to overcome this barrier since combining reverse correlation with calcium imaging would afford a powerful alternative to current methods of measuring response properties of neurons non-invasively in vivo. We labeled zebrafish optic tecta with a calcium indicator and measured responses to a whole-field random flicker light stimulus. Although calcium signals exhibited slow decay kinetics, we could use computational modeling to show that the positive differential of these traces extracts high frequency information. Experimentally, we found that calcium signals processed in this way were synchronous with simultaneously measured synaptic responses and could be used with reverse correlation to determine temporal filters of neurons in the zebrafish optic tectum. These findings demonstrate that calcium responses to physiological stimulation can be processed to obtain rapid signal information and consequently to determine linear filter properties in vivo.

Keywords: Zebrafish; In vivo; Calcium imaging; Reverse correlation; Patch clamp

1. Introduction

Spike-triggered averages and reverse correlation techniques (de Boer and Kuyper, 1968) have been used extensively to study properties of visually responsive neurons in the retina, lateral geniculate nucleus (LGN) and primary visual cortex (de Boer and Kuyper, 1968; Jones and Palmer, 1987; Reid et al., 1997). The responses of neurons at these early stages of visual processing, such as simple cells in primary visual cortex, can be described quite accurately using this approach. Other neurons, like complex cells, can be described by extending this formalism (Touryan et al., 2002). Descriptions of visual responses based on reverse correlation provide an important framework for characterizing response selectivities, a reference point for identifying and characterizing novel effects, and a basis for building mechanistic models (Dayan and Abbott, 2001; Marmarelis, 2004).

In most studies using reverse correlation, the intrinsic limitations of electrophysiological recording have traditionally restricted analyses to single neurons. Meanwhile, a number of techniques have emerged allowing for multicellular response measurements, beginning with multi-electrode recording (Kruger and Bach, 1981). More recently, a notable advance in studying neuronal population activity has been made through the in vivo application of membrane permeant AM Ester calcium indicators (Kerr et al., 2005; Ohki et al., 2005; Sullivan et al., 2005). These studies, while fascinating in their elucidation of response properties in many neighboring neurons, have been technically limited by the intrinsically slow kinetics of measured calcium transients. This constraint forces experimental decisions on the range of possible visual stimuli and lengthens the required duration of fluorescence imaging. Underlying these choices are assumptions about the dynamics, sources, and statistics of evoked signals, which undercut the potential information content of responses. In contrast, reverse correlation methods utilizing random-noise stimuli circumvent these issues by allowing the responses of a neuron to a wide range of stimuli to provide a more accurate description of the neuron's functional properties. While these methods can be more informative, they are thought to be inaccessible to studies using calcium signals for several reasons. Acquisition of a lin-

* Corresponding author. Tel.: +1 617 384 9773; fax: +1 617 495 9300.
E-mail address: ramdya@fas.harvard.edu (P. Ramdya).

0165-0270/$ – see front matter © 2006 Elsevier B.V. All rights reserved.
doi:10.1016/j.jneumeth.2006.04.021

ear filter function requires a substantial minimum of response information. Rapid stimulation necessary for such data acquisition seems to be precluded by the convolution of intrinsic neuronal responses with the long decay kinetics of fluorescence signals. Consequently, reverse correlation of calcium signals would seem to require either prohibitively lengthy experiments prone to phototoxicity and bleaching, or the extraction of temporally rapid signals from a dynamic fluorescence trace. Here we use the latter method to show that reverse correlation of calcium signals is possible in a computational model and experimental recordings in the larval zebrafish in vivo preparation.

The zebrafish, *Danio rerio*, has rapidly become a model system for developmental studies of the vertebrate nervous system (Baier et al., 1996). Genetic tractability, anatomical simplicity, and almost complete transparency also render it a strong candidate for a comprehensive mapping of nervous system function by imaging of neuronal populations (Brustein et al., 2003; Friedrich and Korsching, 1997; Gahtan et al., 2002; Nicolson et al., 1998). One of the most accessible brain regions of the zebrafish is the optic tectum. Analogous to the mammalian superior colliculus, the tectum is thought to process visual information from the environment for use in orienting and tracking movements such as those used in prey capture behavior (Gahtan et al., 2005; Herrero et al., 1998; McElligott and O'Malley, 2005). Tectal neurons primarily receive innervation from retinal ganglion cell (RGCs) axons leaving the contralateral retina (Schwassman and Kruger, 1965). These monosynaptic connections are excitatory and are probably influenced by polysynaptic local inhibitory connections (Sajovic and Levinthal, 1982). Recent work in the larval zebrafish has demonstrated a complete and adult-like retinotopic mapping of response properties in this system (Niell and Smith, 2005).

We examined the amenability and means of using rapid calcium signals from tectal neurons to calculate temporal filters using reverse correlation. To do this, we labeled the tectum with Oregon-Green 488 BAPTA AM Ester (OGB1-AM) and measured visually evoked calcium responses in tectal regions to physiological whole-field random-flicker stimulation. We show that differentiation and positive rectification of calcium signals allows for temporal filter measurement using reverse correlation in the zebrafish optic tectum in vivo.

2. Materials and methods

2.1. Preparation of the zebrafish tectum

Zebrafish larvae between 8 and 10 dpf (days post-fertilization) were raised in fish water (2 g per gallon of Instant Ocean in deionized water) with a 12 h on, 12 h off light cycle. Fish were anaesthetized in 0.02% MS222 (Sigma), pinned to a 35 mm Sylgard dish, and incubated in MMR solution (NaCl 100 mM; KCl 2 mM; $MgSO_4$ 1 mM; $CaCl_2$ 2 mM; EDTA 100 μM; HEPES 5 mM; pH 7.4) containing 100 μM (+)-Tubocurarine (Sigma). Following this, the skin covering the optic tectum was carefully removed, exposing the surface of the tectum and permitting dye application. All animal experiments were approved by Harvard University's standing committee on the use of animals in research and training.

2.2. Calcium indicator loading and imaging

OGB1-AM (Molecular Probes, Eugene, OR) was dissolved at a concentration of 1 mM in DMSO with 20% pluronic acid (Molecular Probes) and diluted to a concentration of 10 μM in MMR. Whole fish with exposed tecta were incubated with this solution for 30 min and subsequently washed with MMR. Neurons were then imaged at 60× magnification on an Olympus Upright Microscope (BX51WI) outfitted with a 75 W Xenon lamp (Opti-Quip) and an OGB filter set (Chroma). Custom designed LabView (National Instruments) programs were used for stimulus design and analysis. Each region of interest (ROI) was approximately 5 μm^2 and restricted to clearly stained somata in the neuropil and cell body layers of the tectum. ROIs were examined for fluorescence changes using a CCD camera (Orca-ER, Hamamatsu) at a 20 Hz frame rate. These measurements were then expressed as a computed $\%\Delta F/F$ value following compensation for photobleaching.

2.3. Visual stimulation

An LED (300 mcd, Radioshack) emitting red wavelength light was placed approximately 3 cm from the retina contralateral to the tectum being examined. The LED voltage fluctuated between constants representing empirically determined maximum (2.5 V) and minimum (1.8 V) intensity values within the linear range of the LED. The protocol used to screen for light responsive neurons consisted of a computer controlled 50 ms maximal LED voltage step. Flicker stimulation consisted of random LED voltage fluctuations anywhere within absolute maximum and minimum intensities at a 20 Hz presentation rate to match the image acquisition frequency.

2.4. Electrophysiology

We measured synaptic currents in zebrafish tectal neurons using whole-cell perforated patch clamp recording methods. Micropipettes made of borosilicate glass capillaries (Kimax) with a resistance of 10–12 MΩ were back-filled with 200 μM Amphoterocin B (Sigma) in internal solution (K-gluconate 110 mM; KCl 10 mM; NaCl 5 mM; $MgCl_2$ 1.5 mM; HEPES 20 mM; EGTA 0.5 mM; pH 7.3). Electrophysiological data were recorded with a patch clamp amplifier (EPC8; HEKA Electronik), filtered at 5 kHz, and sampled at 10 kHz via a data acquisition board (National Instruments) into a PC running LabView. These data were de-noised off-line and binned to 100 Hz for presentation. All data were analyzed using a custom designed LabView program.

2.5. Calcium signal processing

To filter for the onset times of fluorescence transients, we found the first derivative of the raw fluorescence trace (measured $\Delta F/F$ or the difference between successive frames divided

by the mean). Subsequently we applied positive rectification to this differentiated data, removing negative values corresponding principally to signal decay from analysis.

2.6. Cross-correlation

Cross-correlation analyses were computed using LabView by convolving the evaluated traces with one another. The time position of the peak value indicates the delay of correlation between traces. Correlation was normalized to give a correlation probability (CP) value between 0 and 1 (Yoshimura et al., 2005). CP values were computed as shown in Eq. (1). $A1_p$ and $A2_p$ represent the peak values of the autocorrelations of traces $A1$ and $A2$ respectively. C_p indicates the peak value of the cross-correlation between traces $A1$ and $A2$:

$$\mathrm{CP} = \frac{C_p}{\sqrt{(A1_p)(A2_p)}} \tag{1}$$

2.7. Reverse correlation

Reverse correlation analysis can be considered a delineation of the stimulus producing the greatest response in a given neuron. In the visual system this is typically determined in the dimensions of visual space and time in which optimal stimulus characteristics are called spatial and temporal filters respectively. For a clear formalism see Dayan and Abbott (2001) and Marmarelis (2004). In this study, temporal filters were determined by the deconvolution of a random-noise stimulus waveform from resultant neuronal responses, either using post-synaptic currents (PSCs) or processed $\Delta F/F$ signals.

2.8. Modeling neuronal responses

To determine how calcium signals might be processed to allow for accurate temporal filter acquisition by reverse correlation, we developed a model of the linear response of a visually responsive neuron using custom designed LabView software. We generated a white-noise stimulus as described for visual stimulation above and convolved this trace with a mathematically generated OFF filter function waveform (Eq. (2)) whereby t denotes time in milliseconds:

$$f(t) = -5\ \sin(0.000125t)\,\mathrm{e}^{-0.5t} \tag{2}$$

We then convolved this response with a fluorescence filter waveform (Eq. (3)) with a τ of approximately 333 ms. This was derived from the average of experimentally observed calcium transients:

$$f(t) = t^{0.4}\,\mathrm{e}^{-0.00005t} \tag{3}$$

Further processing included positive rectification of the derivative of the fluorescence response. This discarded low frequency information and retained primarily positive deflections of calcium signals describing activity onset times.

2.9. Model assessment

In order to assess how well our modeled calcium signals approximated an ideal estimate of cellular responses before and after processing, we performed regression analyses of these traces. R^2-values were determined using Eq. (4). E_i is the ith value of the evaluated trace (either fluorescence response or processed fluorescence response traces) and R_i is the ith value of the response trace, both of which have n data points. R_m is the mean value of the response trace:

$$1 - \frac{\sum_i^n (E_i - R_i)^2}{\sum_i^n (R_m - R_i)^2} \tag{4}$$

The maximum R^2-value of 1 would indicate that the evaluated trace is identical to the response trace.

3. Results

3.1. Calcium indicator loading and visual stimulation of the larval zebrafish

The larval zebrafish tectum (Fig. 1A) was superficially labeled using OGB1-AM. At the developmental stages examined two prominent tectal layers, the cell body containing superficial paraventricular (SPV) zone and the neurite rich neuropil region, were clearly visible (Fig. 1B). We selected neurons from both areas for analysis in this study. Somata were characterized by higher intensity labeling and a spheroid shape but processes could not be distinguished from background fluorescence (Fig. 1B, inset). The degree of somatic staining was heterogeneous, indicating that neurons may have contained different concentrations of calcium indicator or baseline intracellular calcium. This may have been random, or due in part to phenotypic differences among neurons in intracellular calcium regulation or esterase activity. Empirically we found that less brightly stained cells gave the most robust responses.

Fluorescence measurements were acquired by integrating over small regions of interest within the somata of tectal neurons. In every experiment ($n = 7$), cells were first probed with a series of light flashes each with a 50 ms duration to test for visual responsiveness. In all cases, somatic fluorescence responses exhibited a slow τ (time to half-maximum decay) on the order of 300–500 ms (Fig. 1C). While sometimes non-stimulus locked, the most robust responses were light-evoked. As expected, when a more rapid and complex white-noise random-flicker stimulus was presented to the retina, raw fluorescence responses from the same neurons exhibited more intricate dynamics. A representative trace is shown in Fig. 1D. This is at least in part due to the temporal summation of dynamic amplitude responses to rapid stimuli with varying degrees of contrast fluctuation. When reverse correlation methods were applied to these dynamic fluorescence signals, no temporal filter could be obtained. In contrast, electrophysiological recordings of tectal neurons consistently yield clear temporal filters (data not shown).

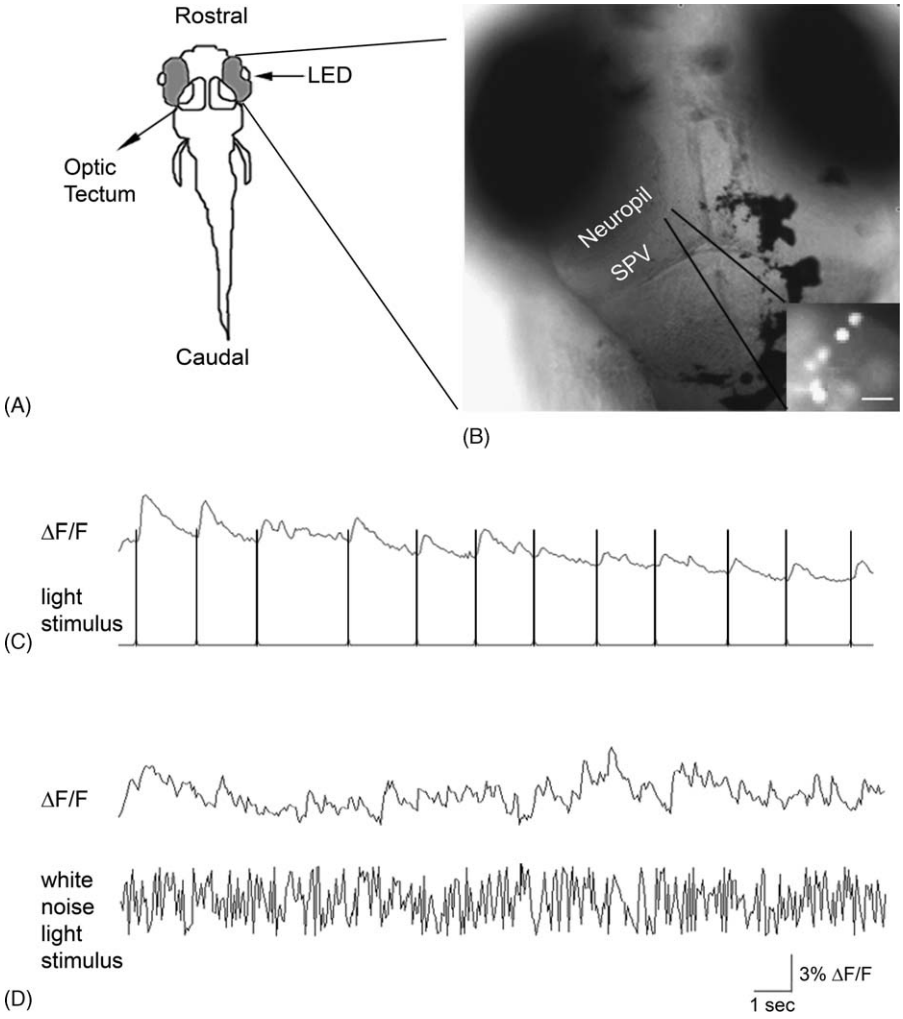

Fig. 1. Zebrafish tectal neuron loading and rapid responses to visual stimulation in vivo. (A) A dorsal schematic of the larval zebrafish and the rostrally situated optic tectum. We presented whole field visual stimuli 3 cm from the retina contralateral to the tectal lobe examined. (B) A transmitted light CCD image of the optic tectal lobes with prominent neuropil and SPV regions labeled. (Inset) Under fluorescent illumination, somata in the tectal neuropil could be clearly discerned as highly fluorescent spheres. Scale bar: (A) 100 μm, (B) 20 μm, (inset) 5 μm. (C) Representative light-evoked calcium signals from a neuron in the neuropil (similar to those in (B)). These signals are reliable, robust, and exhibit long decay kinetics. Non-stimulus evoked signals, while present, are less pronounced. (D) Fluorescence signals in response to a whole field white-noise light stimulus.

3.2. Model of fluorescence signal generation and processing

We hypothesized that an extraction of high frequency response onset information would permit reverse correlation of these slowly decaying fluorescence signals. Briefly, to test this we created a model of a visual neuron's fluorescence response to a whole-field white-noise random flicker stimulus. The model was derived using a known neuronal temporal filter to produce an ideal response trace similar to that obtained from electrophysiological recordings. From a related simulated fluorescence response, we then used signal processing to recover the ideal response trace, and consequently through reverse correlation the neuronal temporal filter.

We began by mathematically convolving a white-noise random-flicker stimulus like that presented experimentally (Fig. 1D) with an approximation (see Section 2 for details) of an 'OFF' temporal filter typically observed from reverse correlation of electrophysiological recordings (Fig. 2A). The function is graphed from 0 ms to more negative time points. A large negative deflection (characteristic of an 'OFF' response) reaches its peak at approximately −100 ms.

Convolution of this temporal filter with a stimulus trace yielded a neuronal response trace. Negative values of this response were then discarded in accordance with the rectified nature of neuronal activity (e.g. the presentation of an 'ON' stimulus to an 'OFF' zebrafish tectal neuron produces no response rather than a negative 'OFF' response). This final trace signifies the model neuron's linear time-varying response. It is reminiscent of an inverted representation of patch-clamp recordings of excitatory post-synaptic currents (EPSCs). Experimentally, when both the response of a neuron and the random (white-noise) whole-field stimulus evoking this response are known, reverse correlation is simply a deconvolution of the stimulus from the response, which yields the neuron's temporal filter. However, in calcium imaging experiments, neuronal responses are further

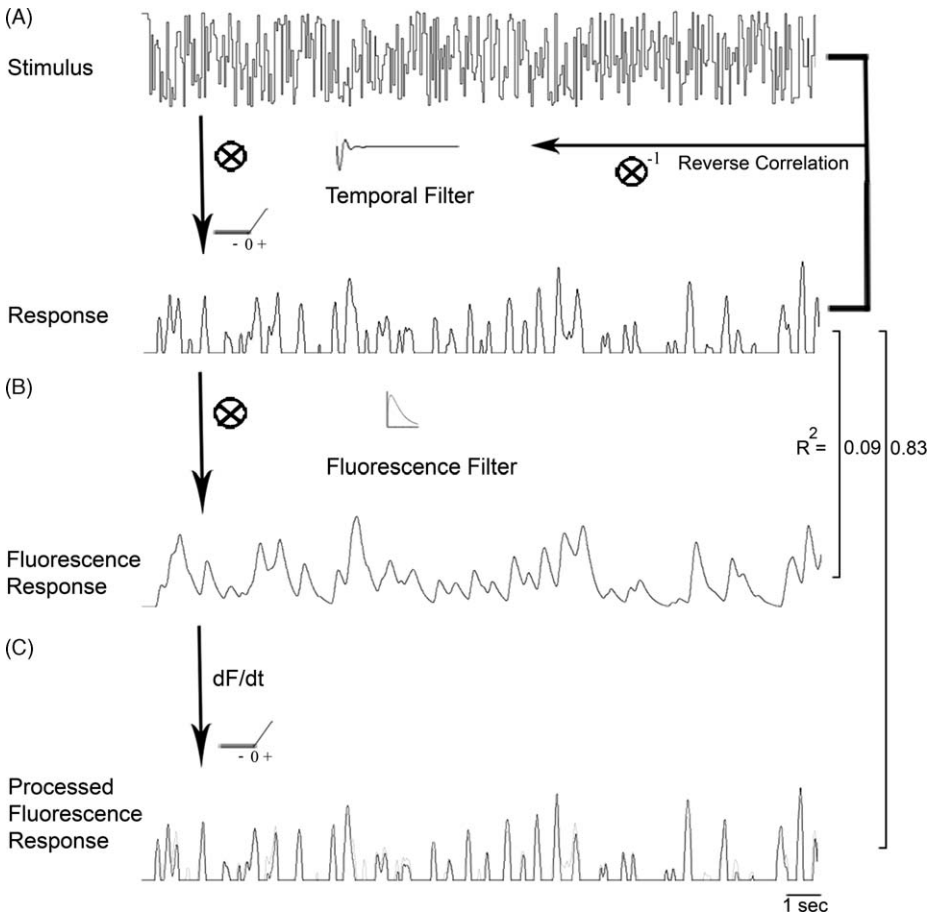

Fig. 2. Modeling responses, reverse correlation, and processing of fluorescence transients. (A) A linear estimate of the response of a model neuron to a white-noise stimulus can be approximated by convolving the stimulus with a temporal filter, in this case an 'OFF' filter, and discarding negative values to resemble predominantly unidirectional current traces. Experimentally, reverse correlation is the inverse of this in that a temporal filter, which describes the linear response characteristics of the recorded neuron, is obtained by deconvolving the known stimulus from the recorded response. (B) An approximation to experimental optical signals is obtained by convolving the response with a slowly decaying waveform (fluorescence filter) representing the putative effect of a calcium indicator on the actual response. This has a low R^2-value, 0.09 (maximum 1.0 for identity), indicating little resemblance with the original response. (C) Differentiating the fluorescence response and positively rectifying it results in a processed fluorescence response (black) which recovers information from and more accurately represents the response (light gray, $R^2 = 0.83$).

convolved with a function relating the indicator's binding kinetics. This additional convolution critically distorts the outcome of reverse correlation and is the issue we sought to address by signal processing.

The effect of a slow indicator dye such as Oregon-Green on the signals generated in our model neuron can be represented by further convolution with an approximation of a decaying fluorescence transient (see Methods for details). The result is the fluorescence response, which approximates calcium imaging traces encountered experimentally. We found that this new response differed dramatically from the original response and had an R^2-value of 0.09 out of a maximum of 1 (Fig. 2B). Our final goal was to derive the original response trace (Fig. 2A) from this fluorescence response.

We reasoned that the distorting effect of the fluorescence filter on the ideal response was mostly due to slow decay kinetics, related by τ in our model since fluorescence onset can be rapid. If τ was brought to extremely small values, the fluorescence filter now resembled a δ function (a function often used to mathematically approximate neuronal spikes). The resultant fluorescence response resembled the original response almost perfectly ($R^2 = 0.99$). This is to be expected since a δ function convolved with any function yields the original function. With real calcium responses, one solution for deriving instantaneous signals most resembling the δ function would be through deconvolution of the calcium signal's impulse response function. Unfortunately, in heterogenous experimental conditions this is difficult to know making this method less than ideal. Instead, to closely emulate this type of decay shortening, we sought to process fluorescence responses to isolate onset information. First we found the differential of the fluorescence response and then positively rectified the resulting signal since negative derivatives or slopes primarily relate the decay of calcium signals. This yielded the processed fluorescence response (Fig. 2C, black), which has a remarkable resemblance to the original response (Fig. 2C, light gray, $R^2 = 0.83$) and yielded the model neuron's temporal filter after reverse correlation.

3.3. Application of signal processing and reverse correlation in vivo

We next sought to determine whether these signal processing techniques could be applied in the larval zebrafish tectum to yield information about rapid calcium responses. First, we examined the relationship between processed optical signals and synaptic events, which are known to directly correlate with spiking events, using electrophysiological recordings. While raw fluorescence signals seemed to be most informative about rare, robust calcium events, the positive differentiated calcium signal was suggestive of many events with a large variance in amplitude. To relate these processed signals to synaptic activity, we simultaneously recorded synaptic currents from a neuron and calcium signals located within its region of interest. Fig. 3A shows 1 min of these current and fluorescence traces during retinal stimulation with a white-noise random-flicker whole field light stimulus. Analogous to findings from the model, processed fluorescence signals and PSCs occur with equal frequency and, surprisingly, exhibit a peak correlation at 0 ms with a high correlation probability (CP) value of 0.34 (Fig. 3B). This relationship continues through 5 min of recording and was confirmed in a second experiment (data not shown). These data emphasize the physiological relevance of processed fluorescence signals (see Section 4).

Reverse correlation of neuronal activity in response to rapid random-noise stimulation is often utilized to measure linear response properties of neurons. Since processed fluorescence signals seemed to extract temporally rapid neuronal response information, we sought to determine if they could be used for measuring temporal tuning properties in the tectum. We found that these signals were sufficient to obtain a temporal

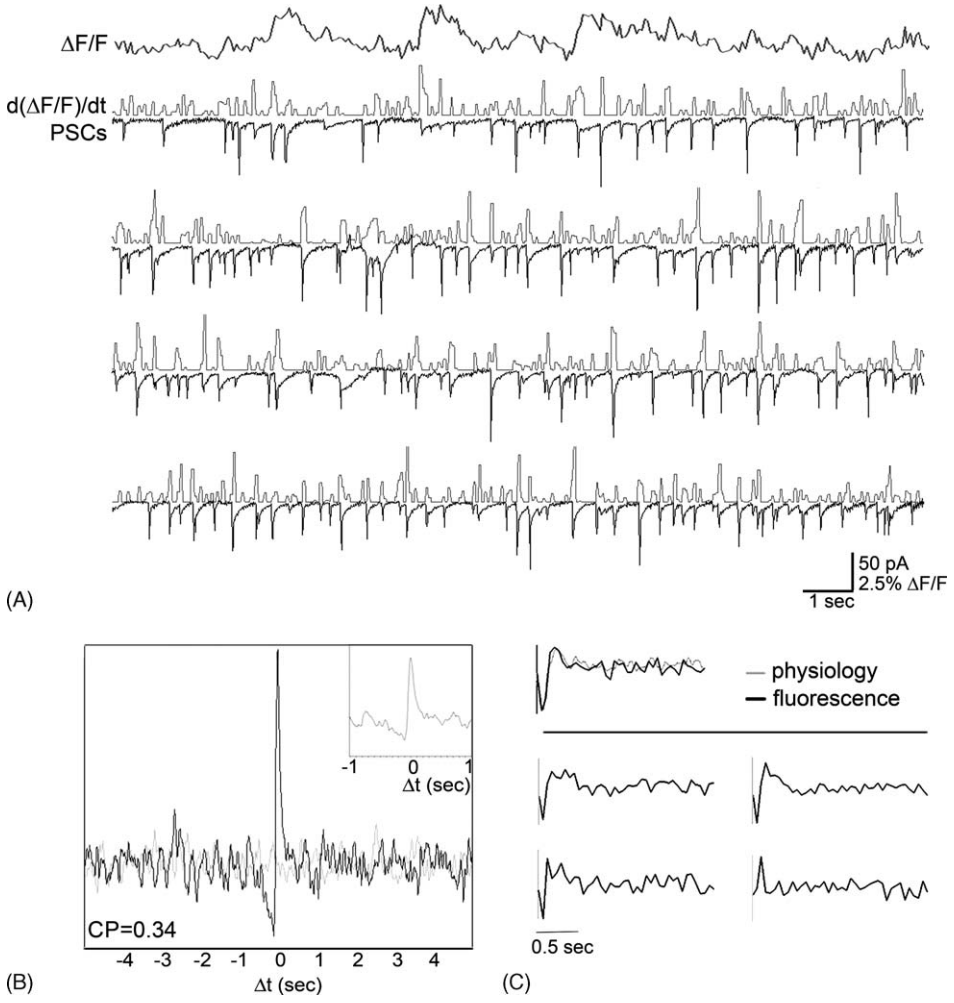

Fig. 3. Processed fluorescence signals closely correlate with synaptic currents and permit reverse correlation in vivo. (A) Raw and processed tectal fluorescence signals are juxtaposed to current traces recorded from a single neuron in the same region of interest in response to a whole field white-noise stimulus. While the raw fluorescence trace ($\Delta F/F$) has little resemblance to the recorded neuron's PSCs, the positive differential of the $\Delta F/F$ signal, $d(\Delta F/F)/dt$, exhibits events which are predominantly simultaneous and occur with similar frequency to those in the voltage-clamp recording. (B) A cross-correlogram of the recorded PSCs and differential fluorescence transients corroborates the coincidence of these signals. A sharp peak with a correlation probability (CP) of 0.34 is present at a Δt of 0 s (black) and absent when one of the data sets is shifted (light gray). The inset is a temporal magnification of this peak. (C, top) Reverse correlation yields similar temporal filters when applied to either processed fluorescence responses (black) or PSCs (light gray). The two filter functions are virtually identical and exhibit a clear 'OFF' response. (C, bottom) Examples of different temporal filters acquired by reverse correlation of processed fluorescence responses in four other experiments. Variable 'OFF' filters and a single 'ON' filter are represented.

filter ($n = 7$). In the case described earlier, as expected from the tight correlation observed, simultaneously recorded PSCs and processed fluorescence responses yield almost identical filter functions, accentuating the utility of our method (Fig. 3C, top). Examples of other temporal filters from separate experiments using only processed calcium signals include diverse 'OFF' and 'ON' temporal filters (Fig. 3C, bottom).

4. Discussion

Neuronal calcium signals can be dissected into two components. The first, signal onset, is most closely related to neuronal responses, be they from action potentials or excitatory synaptic activity. In our system, it is not surprising that EPSCs can closely mimic calcium signals that are typically a result of spiking events (Niell and Smith, 2005) since these two responses are related by a thresholding function that we have found to lie close to the resting potential in zebrafish tectal neurons (data not included). The second component of the calcium signal, the slow decay, is a consequence of calcium indicator binding kinetics. This means that when the differential of a calcium signal trace is taken, the positive derivative denotes the onset of neuronal activity and negative deflections are primarily indicative of decay kinetics. Therefore the positive differential is most informative of neuronal activity. Here we have demonstrated that this positive differential of slowly-decaying fluorescence signals evoked by rapid physiological stimulation can provide an accurate representation of neuronal activity in a mathematical model. This finding was corroborated by calcium imaging in the larval zebrafish tectum in vivo. While a similar method of optical signal processing has been demonstrated previously to describe the onset of action potential bursts in cortical slices (Ikegaya et al., 2004), we demonstrate the utility of this method for delineating rapid time-scale fluorescence signals in vivo. It should be noted that light scattering in thick tissue makes it difficult to pinpoint the precise source of these signals as they may result from the combined activity of several nearby neurons. It is therefore also difficult to say whether the calcium transients are caused by synaptic activation alone or by action potentials (Niell and Smith, 2005).

Notably, we show that calcium signals processed in this way can be utilized for filter function computation. When combined with two-photon imaging, this novel combination of calcium signal processing and reverse correlation could offer a new way of procuring sophisticated information about multi-cellular response properties. Studies investigating the activity of populations of neurons in vivo are clearly becoming the rule as opposed to the exception. In many cases, as in recent pioneering work examining boundaries of orientation selectivity in the mammalian visual cortex (Ohki et al., 2005), distinguishing subtle functional differences between neighboring neurons has become an important problem seeking analytical tools. We propose that the demonstrated methods of merging calcium signal processing with reverse correlation could help in this task by eliminating stimulation biases and permitting powerful population analyses, aiding in the task of understanding the coding of neuronal ensembles in intact organisms.

This novel combination of techniques is poised to be especially useful in studies of the larval zebrafish brain, a model system that continues to be the focus of a large number of studies. Functional analyses of potentially informative mutants including those with retinotectal projection malformations (Baier et al., 1996) have yet to be completed and could yield significant insight into the influence of genetic modulation on the development of circuit function. Additionally, relevant physiological stimuli for various, as of yet, only coarsely understood zebrafish brain nuclei (Gahtan and Baier, 2004) might be uncovered in this manner. Revealing the coding hierarchies within and between brain regions could elucidate information processing from sensory neural circuitry to behavioral output.

Acknowledgements

We thank Drs. C. Reid and M. Meister for critically reading and providing helpful comments during the preparation of this manuscript. This work was supported by a National Defense Science and Engineering Graduate Fellowship to PR and National Institutes of Health grant R01 EY014429-01A2 as well as generous funding from the Klingenstein Foundation to FE.

References

Baier H, Klostermann S, Trowe T, Karlstrom RO, Nusslein-Volhard C, Bonhoeffer F. Genetic dissection of the retinotectal projection. Development 1996;123:415–25.

Brustein E, Marandi N, Kovalchuk Y, Drapeau P, Konnerth A. "In vivo" monitoring of neuronal network activity in zebrafish by two-photon Ca(2+) imaging. Pflug Arch 2003.

Dayan P, Abbott LF. Theoretical neuroscience. MIT Press; 2001.

de Boer E, Kuyper P. Triggered correlation. IEEE Trans Biomed Eng 1968;15:169–79.

Friedrich RW, Korsching SI. Combinatorial and chemotropic odorant coding in the zebrafish olfactory bulb visualized by optical imaging. Neuron 1997;18:737–52.

Gahtan E, Baier H. Of lasers, mutants, and see-through brains: functional neuroanatomy in zebrafish. J Neurobiol 2004;59:147–61.

Gahtan E, Sankrithi N, Campos JB, O'Malley DM. Evidence for a widespread brain stem escape network in larval zebrafish. J Neurophysiol 2002;87:608–14.

Gahtan E, Tanger P, Baier H. Visual prey capture in larval zebrafish is controlled by identified reticulospinal neurons downstream of the tectum. J Neurosci 2005;25:9294–303.

Herrero L, Rodriguez F, Salas C, Torres B. Tail and eye movements evoked by electrical microstimulation of the optic tectum in goldfish. Exp Brain Res 1998;120:291–305.

Ikegaya Y, Aaron G, Cossart R, Aronov D, Lampl I, Ferster D, et al. Synfire chains and cortical songs: temporal modules of cortical activity. Science 2004;304:559–64.

Jones JP, Palmer LA. An evaluation of the two-dimensional Gabor filter model of simple receptive fields in cat striate cortex. J Neurophysiol 1987;58:1233–58.

Kerr JN, Greenberg D, Helmchen F. Imaging input and output of neocortical networks in vivo. Proc Natl Acad Sci USA 2005;102:14063–8.

Kruger J, Bach M. Simultaneous recording with 30 microelectrodes in monkey visual cortex. Exp Brain Res 1981;41:191–4.

Marmarelis VZ. Non-linear dynamic modeling of physiological systems. 1st ed Wiley-IEEE Press Series on Biomedical Engineering; 2004.

McElligott MB, O'Malley DM. Prey tracking by larval zebrafish: axial kinematics and visual control. Brain Behav Evol 2005;66:177–96.

Nicolson T, Rusch A, Friedrich RW, Granato M, Ruppersberg JP, Nusslein-Volhard C. Genetic analysis of vertebrate sensory hair cell

mechanosensation: the zebrafish circler mutants. Neuron 1998;20:271–83.

Niell CM, Smith SJ. Functional imaging reveals rapid development of visual response properties in the zebrafish tectum. Neuron 2005;45:941–51.

Ohki K, Chung S, Ch'ng YH, Kara P, Reid RC. Functional imaging with cellular resolution reveals precise micro-architecture in visual cortex. Nature 2005:433.

Reid RC, Victor JD, Shapley RM. The use of m-sequences in the analysis of visual neurons: linear receptive field properties. Visual Neurosci 1997;14:1015–27.

Sajovic P, Levinthal C. Visual response properties of zebrafish tectal cells. Neuroscience 1982;7:2427–40.

Schwassman HO, Kruger L. Organization of the visual projection upon the optic tectum of some freshwater fish. J Comp Neurol 1965;124:113–26.

Sullivan MR, Nimmerjahn A, Sarkisov DV, Helmchen F, Wang SS. In vivo calcium imaging of circuit activity in cerebellar cortex. J Neurophysiol 2005;94:1636–44.

Touryan J, Lau B, Dan Y. Isolation of relevant visual features from random stimuli for cortical complex cells. J Neurosci 2002;22:10811–8.

Yoshimura Y, Dantzker JL, Callaway EM. Excitatory cortical neurons form fine-scale functional networks. Nature 2005;433:868–73.